

LETTER TO THE EDITOR

HIP 41378 observed by CHEOPS: Where is planet d?★,★★

S. Sulis¹, L. Borsato², S. Grouffal³, H. P. Osborn^{4,5}, A. Santerne³, A. Brandeker⁶, M. N. Günther⁷, A. Heitzmann⁸, M. Lendl⁸, M. Fridlund^{9,10}, D. Gandolfi¹¹, Y. Alibert^{4,12}, R. Alonso^{13,14}, T. Bérczy¹⁵, D. Barrado Navascués¹⁶, S. C. C. Barros^{17,18}, W. Baumjohann¹⁹, T. Beck¹², W. Benz^{12,4}, M. Bergomi²⁰, N. Billot⁸, A. Bonfanti¹⁹, C. Broeg^{12,4}, A. Collier Cameron²¹, C. Corral van Damme⁷, A. C. M. Correia²², Sz. Csizmadia²³, P. E. Cubillos^{24,19}, M. B. Davies²⁵, M. Deleuil¹, A. Deline⁸, L. Delrez^{26,27,28}, O. D. S. Demangeon^{17,18}, B.-O. Demory^{4,12}, A. Derekas²⁹, B. Edwards³⁰, D. Ehrenreich^{8,31}, A. Erikson²³, A. Fortier^{12,4}, L. Fossati¹⁹, K. Gazeas³², M. Gillon²⁶, M. Güdel³³, Ch. Helling^{19,34}, S. Hoyer¹, K. G. Isaak⁷, L. L. Kiss^{35,36}, J. Korth³⁷, K. W. F. Lam²³, J. Laskar³⁸, A. Lecavelier des Etangs³⁹, D. Magrin², P. F. L. Maxted⁴⁰, C. Mordasini^{12,4}, V. Nascimbeni², G. Olofsson⁶, R. Ottensamer³³, I. Pagano⁴¹, E. Pallé^{13,14}, G. Peter⁴², D. Piazza⁴³, G. Piotto^{2,44}, D. Pollacco⁴⁵, D. Queloz^{46,47}, R. Ragazzoni^{2,44}, N. Rando⁷, H. Rauer^{23,48}, I. Ribas^{49,50}, N. C. Santos^{17,18}, G. Scandariato⁴¹, D. Ségransan⁸, A. E. Simon^{12,4}, A. M. S. Smith²³, S. G. Sousa¹⁷, M. Stalport^{27,26}, M. Steinberger¹⁹, Gy. M. Szabó^{51,52}, A. Tuson⁵³, S. Udry⁸, S. Ulmer-Moll⁸, V. Van Grootel²⁷, J. Venturini⁸, E. Villaver^{13,14}, N. A. Walton⁵³, T. G. Wilson⁴⁵, D. Wolter²³, and T. Zingales^{44,2}

(Affiliations can be found after the references)

Received 21 February 2024 / Accepted 28 May 2024

ABSTRACT

HIP 41378 d is a long-period planet that has only been observed to transit twice, three years apart, with K2. According to stability considerations and a partial detection of the Rossiter–McLaughlin effect, $P_d = 278.36$ d has been determined to be the most likely orbital period. We targeted HIP 41378 d with CHEOPS at the predicted transit timing based on $P_d = 278.36$ d, but the observations show no transit. We find that large (>22.4 h) transit timing variations (TTVs) could explain this non-detection during the CHEOPS observation window. We also investigated the possibility of an incorrect orbital solution, which would have major implications for our knowledge of this system. If $P_d \neq 278.36$ d, the periods that minimize the eccentricity would be 101.22 d and 371.14 d. The shortest orbital period will be tested by TESS, which will observe HIP 41378 in Sector 88 starting in January 2025. Our study shows the importance of a mission like CHEOPS, which today is the only mission able to make long observations (i.e., from space) to track the ephemeris of long-period planets possibly affected by large TTVs.

Key words. planets and satellites: individual: HIP 41378

1. Introduction

The bright F-type star HIP 41378 ($m_V \approx 8.9$; $T_{\text{eff}} = 6290 \pm 77$ K; Lund et al. 2019) is transited by at least five exoplanets (Vanderburg et al. 2016) with very long orbital periods, up to 1.5 yr for planet f (Santerne et al. 2019). With this period, the transit probability is as low as 0.4%. The planetary system transiting HIP 41378 is thus a unique laboratory for studying the compositions and atmospheres of planets that are not extremely irradiated, and which fall in the gap between the cold outer Solar System planets and hot gaseous planets. It is also an interesting system to search for moons and rings, in particular around planet f (see, e.g., Akinsanmi et al. 2020; Saillenfest et al. 2023; Belkovski et al. 2022; Alam et al. 2022; Edwards et al. 2023; Harada et al. 2023).

In this system, planet d has been seen to transit twice, three years apart, in photometric data from the K2 mission, during Campaign 5 (Vanderburg et al. 2016) and Campaign 18 (Berardo et al. 2019; Becker et al. 2019). This resulted in 23 possible period aliases: namely, 3 yr and all the harmonics down to about 50 days, which is the size of the continuous window of observations. Combining the long transit duration ($t_{\text{dur}} \approx 12.5$ h) and the precise and accurate density of the host star derived thanks to asteroseismology, Lund et al. (2019) estimate that the most likely orbital period for planet d that minimizes the eccentricity in this massive multi-planet system is $P_d = 278.36 \pm 0.001$ d.

The star HIP 41378 was also intensively observed via radial velocity (RV), mainly with the HARPS (Mayor et al. 2003) and HARPS-N (Cosentino et al. 2012) spectrographs. However, no significant RV signal was found at ~ 278 d by Santerne et al. (2019); possibly because the signal may have been too faint for the stability of these instruments (small periodicities at ~ 350 – 410 days are, however, reported in their RV data analyses). The star was recently photometrically monitored by the TESS space telescope over seven sectors, but no transit of planet

* The raw and detrended photometric time-series data are available at the CDS via anonymous ftp to cdsarc.cds.unistra.fr (130.79.128.5) or via <https://cdsarc.cds.unistra.fr/viz-bin/cat/J/A+A/686/L18>

** The CHEOPS program ID is CH_PR110048.

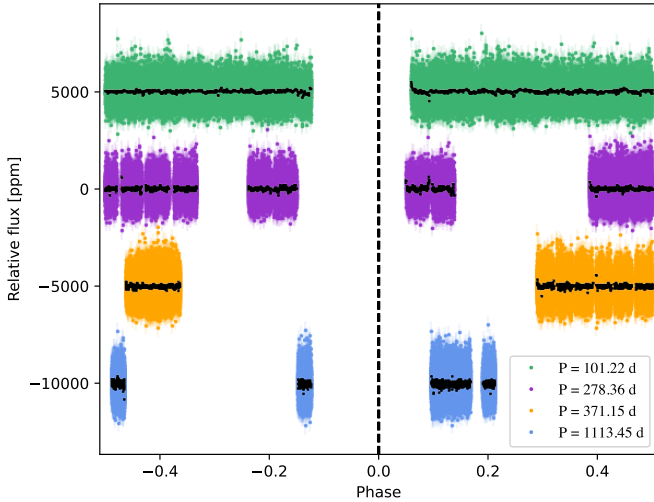


Fig. 1. TESS observations of HIP 41378 (sectors 7, 34, 44, 45, 46, 61, and 72) phase-folded at different orbital periods (see the legend). 3-h-binned data are shown in black. The different series have been shifted in flux for visibility. The transit duration is within the thickness of the vertical line.

d was detected (see Fig. 1) despite an expected S/N above 400. These TESS observations allowed 16 of the 23 orbital period aliases inferred after the K2 campaign for planet d to be discarded (see Grouffal et al. 2022); the value $P_d = 278.36$ d remained the most plausible.

Given its long duration and shallow depth (650 ppm), the transit is challenging to detect using ground-based facilities. Instead, Grouffal et al. (2022) used high-resolution spectroscopy and detected a signal compatible with an egress of the Rossiter–McLaughlin (RM) effect (Holt 1893; Rossiter 1924; McLaughlin 1924) at the expected transit time and with an amplitude compatible with the ~ 278 d period, providing evidence in support of this orbital solution.

Assuming the orbital period of ~ 278 d is accurate, we observed HIP 41378 with CHEOPS (Benz et al. 2021) at the expected transit timing of planet d ($T_{0,d} = 2459949.8787 \pm 0.008$; Grouffal et al. 2022), which represented the only transit event visible in both the nominal and first extended CHEOPS mission. With this, we aimed to confirm the planet’s orbital period and to constrain possible transit-timing variations (TTVs) of HIP 41378 d, as observed for planet f (Bryant et al. 2021). These objectives are in line with results from other CHEOPS programs that have confirmed moderately long-period planets, for example TOI-2076c (Osborn et al. 2022), HIP 9618c (Osborn et al. 2023), TOI-5678b (Ulmer-Moll et al. 2023), HD22946d (Garai et al. 2023), HD15906b and c (Tuson et al. 2023), and TOI-815c (Pсариди et al. 2024). This Letter reports on the CHEOPS observations of HIP 41378 and discusses their implications for the system characterization.

2. CHEOPS observations and analysis

The CHEOPS visit of HIP 41378 was scheduled as part of the guaranteed time observing program. HIP 41378 was observed for $T_{\text{WIN}} = 32.3$ h from January 4, 2023, at T16:14:16 to January 6, 2023, at T00:32:21 UTC. The integration time of each measuring point was ~ 38 s. During these observations, the duty cycle was close to 61%. The origin of the data gaps lies in the low-Earth orbit of CHEOPS: when the satellite crosses the South Atlantic Anomaly, when the Earth occults the target, or when

stray light contamination is too high, data are not downloaded (Benz et al. 2021). A summary of CHEOPS HIP 41378 observations is presented in Table 1. Observations were processed with the automatic CHEOPS Data Reduction Pipeline (DRP; v14.1.2), described in Hoyer et al. (2020). We adopted the target flux obtained with the default radius aperture, which is $r = 25$ pixels. Two main contaminants are present in this photometric aperture, but they are faint (G -mag = 14 and 18.2) compared to the target (G -mag = 8.81). The “raw” light curve, obtained by removing outliers exceeding 5σ (11 data points), is presented in the top panel of Fig. 2.

We detrended the light curve from instrumental and environmental noise using the python package `pycheops`¹ (Maxted et al. 2022). To de-correlate the light curve from CHEOPS systematics, we first identified the relevant parameters using the `should_I_decorr()` function of `pycheops`. This function fits various combinations of trends between flux, time, roll angle (Φ), and the different variables provided by DRP (e.g., target centroid positions, background, contamination flux, and smear contamination). For each combination, it calculates the Bayesian information criterion (BIC) and determines the combination that yields the lowest BIC value (see Sect. 2 of Maxted et al. 2022 for details). We find that the best-fitting combination of detrending parameters involves the first- and second-order derivative in time ($d\text{fd}t$ and $d^2\text{fd}t^2$), the first- and second-order derivative of the offset in the x and y centroid positions ($d\text{fd}x$, $d^2\text{fd}x^2$, $d\text{fd}y$, and $d^2\text{fd}y^2$), the first three harmonics of the roll angle (in $\cos \Phi$ and $\sin \Phi$), and linear trends with the sky background ($d\text{fdbg}$), contamination ($d\text{fdcontam}$), and smearing systematics ($d\text{fdsmear}$). The root mean square of the light curve before and after this de-correlation step is 523 and 271 ppm, respectively. The final light curve is shown in Fig. 2. No transit is detected at the predicted ephemeris $T_{0,d}$ calculated by Grouffal et al. (2022) assuming an orbital period of $P_d = 278.36$ d and a transit depth of 650 ppm (Vanderburg et al. 2016).

3. Discussion: Where is planet d?

We devised two main hypotheses to explain the non-detection of the transit of HIP 41378 d in the CHEOPS light curve. They are as follows.

3.1. Possible large TTV signal

Assuming the alias at $P_d \sim 278$ d and the Santerne et al. (2019) solution are correct, we dynamically integrated the whole system with TRADES² (Borsato et al. 2014, 2019, 2021). The solution in Santerne et al. (2019) was the result of the sum of noninteracting Keplerian orbits, so it provides a mean orbital configuration without knowledge of the exact position of all the planets at some reference time.

Under these conditions, we had to take the values of the initial parameters based on the Santerne et al. (2019) solution. We calculated $M = \frac{2\pi}{P}(t_{\text{ref}} - \tau)$, where t_{ref} is the transit time of planet d in Campaign 18 of K2 and τ is the time of passage at pericenter. For planet d we assumed $M_d(t_{\text{ref}}) = 0^\circ$, and for the other five planets we assigned random values between 0° and 360° . We assumed the argument of the pericenters (ω) to be 90° for all the planets. We integrated the orbits of the six planets for 200 yr and extracted the synthetic transit times ($T_{0,s}$)

¹ <https://github.com/pmated/pycheops> (version 1.1.7).

² <https://github.com/lucaborsato/trades>

Table 1. Log file of CHEOPS observations: file keys referring to the files name in the CHEOPS database, starting date (BJD), total observation duration, number of data points before and after detrending, number of CHEOPS orbits, duty cycle (DC), and exposure time.

File key in the CHEOPS database	Starting date (BJD)	Duration (h)	Data points (raw/detrended)	# orbits	DC (%)	Exposure time (s)
CH_PR110048_TG032601_V0300	2459949.183	32.3	1838 / 1827	20	61	38

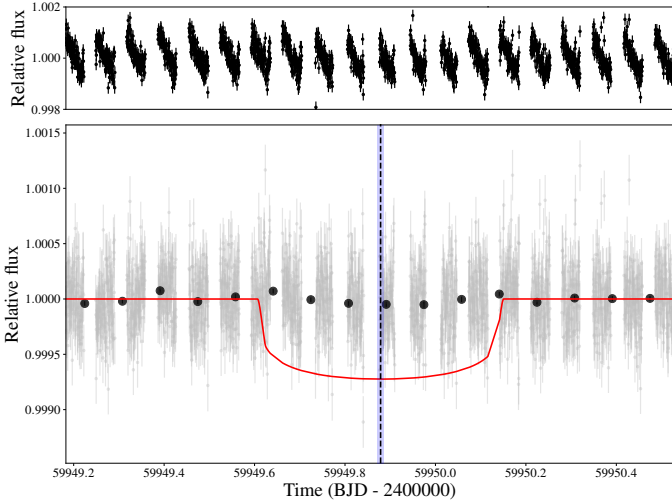


Fig. 2. CHEOPS observations of HIP 41378 at the predicted time of planet d's transit. Top: Raw light curve. Bottom: Detrended (gray) and 2-h-binned light curves (black). The transit model is in red. The dotted vertical line indicates the predicted time of mid-transit $T_{0,d}$, assuming an orbital period of $P_d = 278.36$ d. The shaded blue region represents the uncertainties on $T_{0,d}$.

from the simulation. We exploited the possible TTV signal by constructing an observed minus calculated ($O-C$) diagram: the O is the synthetic $T_{0,s}$ (the initial reference time is the median T_0 and the period is the median of the difference of successive $T_{0,s}$), and the C is a linear ephemeris computed on the synthetic $T_{0,s}$. The amplitude of the synthetic TTV, A_{TTV} , computed as the semi-amplitude of the $O-C$, is approximately 23.55 days over a temporal baseline of 200 yr (see Fig. 3). However, our observational baseline covers only 7.8 yr (from K2 to CHEOPS). Therefore, we started with a temporal window spanning 7.8 yr and shifted it by one transit at a time; by selecting the $T_{0,s}$ that fall in that time range, we recomputed the $O-C$ after refitting the linear ephemeris. The A_{TTV} was derived for each moving window, revealing that the potential TTV signal in the observation windows of the Santerne et al. (2019) orbital configuration can vary from a minimum of $A_{TTV,min} \sim 2$ h to a maximum of $A_{TTV,max} \sim 1$ day (see an example in Fig. 3).

To reduce computational time, we decided to simulate only the three outer planets (d, e, and f), repeating the orbital integration and sliding TTV. This approach yielded comparable results. So we assumed that the effect of the three inner planets is negligible for the purpose of our sliding TTV analysis. We ran 10 000 simulations with TRADES, varying the parameters based on the uncertainty and upper bounds³ proposed by Santerne et al. (2019). We set the lower limit of masses to $0.1 M_{\oplus}$ and forced

³ We could not sample from the posterior (which would have allowed us to conserve the covariance between parameters) because it was no longer available. We had to rely on the marginalized parameter values and uncertainties reported in Santerne et al. (2019).

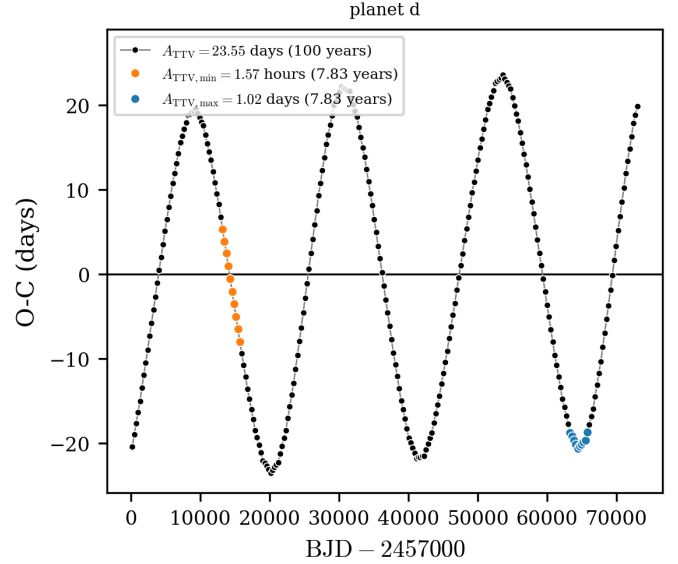


Fig. 3. $O-C$ diagram of synthetic transit times ($T_{0,s}$) of 100 yr (black circles) of dynamical simulations with TRADES computed using the Santerne et al. (2019) solution and including all planets. Highlighted are the two observing windows of ~ 7.8 yr whose re-computed $O-C$ (as described in Sect. 3.1) show the minimum (orange) TTV amplitude ($A_{TTV,min} = 1.57$ h) and the maximum (blue) TTV amplitude ($A_{TTV,max} = 1.02$ days).

only positive eccentricities. The argument of pericenters (ω) of all planets and the mean anomaly (M) of planets e and f were assigned random values between 0° and 360° , the M_d was fixed to 0° , and the longitude of the ascending node (Ω) was set to 180° for all planets. For each simulation, we integrated for 200 yr and computed the sliding TTV. Out of 10 000 simulations, 7 921 (79.21%) were stable over 200 yr. Of these, 3 438 (43.40% of stable simulations and 34.38% of all the simulations) had at least one TTV window above the required threshold of $(T_{WIN} + t_{dur})/2 = 22.4$ h.

This shows that $P_d = 278.36$ d could be the true orbital period of planet d, despite the lack of a transit in the CHEOPS light curve. This is compatible with the RM detection reported in Grouffal et al. (2022). However, it would imply that our CHEOPS observations were carried out during a particular configuration of the system with an $A_{TTV} > 22.4$ h.

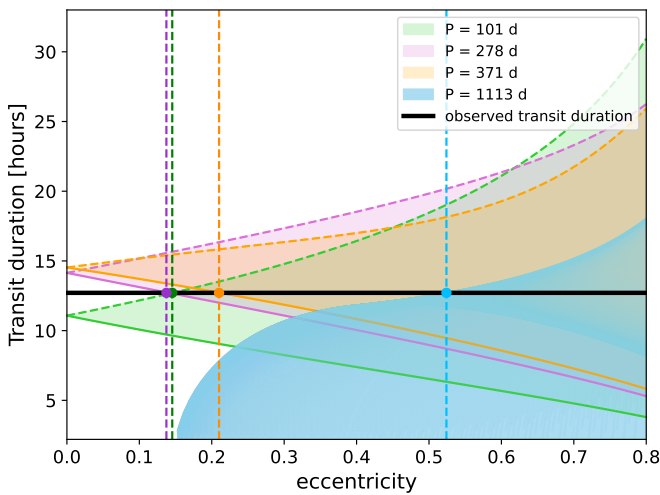
3.2. A different period for planet d

The second scenario is an incorrect orbital period solution for HIP 41378 d. Combining the results of the seven TESS sectors and the new result obtained by CHEOPS, three solutions are possible for the planetary orbital period, as presented in Table 2: 101.22 d, 371.15 d, and 1 113.44 d. None of these three solutions are compatible with the RM detection reported in Grouffal et al. (2022). Many sources of error might have led to a false detection

Table 2. Summary of the remaining orbital periods for HIP 41378 d (assuming no TTV).

Orbital period [d]	TESS	CHEOPS	RM	e_{\min}
1113.4465 ± 0.0034	✓	✓	✗	~ 0.52
371.1488 ± 0.0011	✓	✓	✗	~ 0.21
278.3616 ± 0.0009	✓	✗	✓	~ 0.14
101.2224 ± 0.0003	✓	✓	✗	~ 0.15

Notes. Orbital solutions compatible with no transit in TESS and CHEOPS observations are shown with a check mark (✓), while those incompatible are shown with an ✗. Orbital period values are taken from Becker et al. (2019). The RM column corresponds to the results in Grouffal et al. (2022) for the RM detection of the transit. The last column displays the minimal eccentricity that corresponds to $t_{\text{dur}} \approx 12.5$ h.

**Fig. 4.** Transit duration for eccentricities from 0 to 0.8 for HIP 41378 d for four orbital periods (see the legend). The dotted vertical lines represent the minimal eccentricity for each orbital period to obtain the observed transit duration of 12.5 h (thick black horizontal line).

of the RM effect (e.g., instrumental systematics, stellar variability, and distortion of the RV after the detrending of the data). If the orbital period of 278.36 d turns out to be wrong, it would be interesting to understand the origin of the RM-like signal observed by Grouffal et al. (2022) for future RM analyses of this iconic system.

For each of these periods, we estimated the minimal eccentricity required to observe a transit duration of $t_{\text{dur}} \approx 12.5$ h using Eqs. (7) and (14) from Winn (2010). We used the values from Santerne et al. (2019) for the radius and inclination. We used both the formula for the transit duration from Winn (2010) and that from Kipping (2010), and we obtained similar results. The expected transit duration for the four possible orbital periods as a function of the eccentricities and for ω ranging from periastron to apastron is represented in Fig. 4. The period that minimizes the eccentricity is $P_d = 278.36$ d, which was one of the reasons this orbital period was considered the most plausible. This period is compatible with Lund et al. (2019)’s analysis. An orbital period of 101.22 d with the planet seen at apastron also gives a low eccentricity similar to the one for $P_d = 278.36$ d. Period $P_d = 371.15$ d is also compatible with a reasonable minimal eccentricity of ~ 0.21 . Only period 1113.44 d seems excluded as a high eccentricity is necessary (~ 0.52). We note the different behavior of the transit duration for $P_d = 1113.44$ d

in Fig. 4, which is explained by impact parameters becoming close to or larger than 1 for some eccentricity values in Eq. (7) of Winn (2010).

HIP 41378 is planned to be observed again by TESS during Sector 88 (from January 14 to February 11, 2025), for which a transit of planet d might be detected only if $P_d = 101.22$ d. If $P_d = 278.36$, the next opportunity to detect a transit with CHEOPS will be in January 2026. If $P_d = 371.14$ d or 1113.44 d, there is no opportunity to observe any transit in the next 15 yr with HST, TESS, CHEOPS, or ARIEL.

These new possible period estimates change our view of the HIP 41378 planetary system. Planet e was observed only once in transit during K2’s C5 campaign, with a transit duration of ~ 13 h. Using a global analysis of K2 transits with RV data, Santerne et al. (2019) found an orbital period of $P_e = 369 \pm 10$ d. Using HIP 41378 d’s new orbital period constraints, the period of planet e may be different (especially if $P_d = 371.14$ d or 1113.44 d). Detecting additional transits of planets e and d is necessary to understand these long-period planets.

4. Conclusions

We observed HIP 41378 with CHEOPS for 32.3 h to refine the ephemeris of planet d and constrain the TTVs in order to dynamically analyze the whole system (Santerne et al. 2019). Planet d was first seen to transit twice with K2 (Vanderburg et al. 2016; Berardo et al. 2019; Becker et al. 2019). TESS observations enable one to rule out several period aliases computed after the K2 campaign and are compatible with four period aliases, namely $P_d \sim 101$, 278, 371, and 1113 d. Of these values, $P_d \sim 278$ d was believed to be the most likely period when taking the RM observations by Grouffal et al. (2022) into account.

CHEOPS observations, planned at $P_d \sim 278$ d, showed no transit. The expected S/N of this event rules out a missed planet detection with CHEOPS due to instrumental systematics. Two possible scenarios are discussed in this Letter.

The first scenario assumes that the planet orbital period of $P_d \sim 278$ d is correct but that the transit was not seen due to a large TTV (>22.4 h). With our simulations, we indeed find configurations where $A_{\text{TTV}} > 22.4$ h. Detecting the planet from ground-based observations (with windows of <10 h) would therefore be challenging. We note that the current TTV analysis could benefit from significant refinement from an updated orbital solution of this multi-planet system. We also emphasize the importance of considering dynamical constraints in future RV analyses of this system, which are needed to assign a robust probability to the TTV scenario.

The second scenario assumes that the period solution of ~ 278 d is incorrect. This would not be consistent with the results of Grouffal et al. (2022) and would mean that Grouffal et al. (2022) misinterpreted the RM-like signal. If we consider a different period for planet d, this would change the derived period of the mono-transit of planet e. A complete reanalysis of the RV data is needed, but this goes beyond the scope of this Letter.

In conclusion, CHEOPS observations do not allow us to conclude which of the four possible orbital periods for planet d is correct. However, two periods (namely $P_d \sim 101$ d and 371 d) seem to be possible alternatives as they minimize the planet’s eccentricity and would imply that the CHEOPS observations were made in the $A_{\text{TTV}} < 22.4$ h configuration. Future observations by TESS (Sector 88) will enable us to draw conclusions about the $P_d \sim 101$ d period.

We note that other factors could explain this non-detection, such as the variation in the inclination, which could

make the transit event disappear on a short timescale (e.g., from Saillenfest et al. 2023, the precession period would be $\sim 1000\text{--}2500$ yr). Such a scenario would be interesting to investigate when a more reliable orbital solution for the system becomes available.

This study shows the importance of monitoring long-period planets to keep track of and refine their ephemerides, which may be affected by large TTVs. It may then be necessary to carry out long-duration observations (i.e., from space) around the predicted planet ephemeris to secure the transit detection. The CHEOPS mission, designed to characterize known exoplanets, is particularly well suited to this task. With the future PLATO space mission (scheduled for 2026; Rauer et al. 2014), the discovery of long-period planets should intensify. Consequently, extending the CHEOPS mission post-PLATO launch and/or considering the development of additional CHEOPS-like missions, potentially stationed at L2 (to reduce pointing constraints and time gaps), would be fully justified.

Acknowledgements. The authors thank the anonymous referee for her/his helpful comments that improved this Letter. CHEOPS is an ESA mission in partnership with Switzerland with important contributions to the payload and the ground segment from Austria, Belgium, France, Germany, Hungary, Italy, Portugal, Spain, Sweden, and the United Kingdom. The CHEOPS Consortium would like to gratefully acknowledge the support received by all the agencies, offices, universities, and industries involved. Their flexibility and willingness to explore new approaches were essential to the success of this mission. CHEOPS data analysed in this article will be made available in the CHEOPS mission archive (https://cheops.unige.ch/archive_browser/). S.S. and M.D. acknowledge support from CNES, as well as the Programme National de Planétologie (PNP) of CNRS-INSU. L.B., G.B., V.N., I.P., G.P., R.R., G.S., V.S., and T.Z. acknowledge support from CHEOPS ASI-INAF agreement n. 2019-29-HH.0. This work has been carried out within the framework of the NCCR PlanetS supported by the Swiss National Science Foundation under grants 51NF40_182901 and 51NF40_205606. A.B. was supported by the SNSA. M.N.G. is the ESA CHEOPS Project Scientist and Mission Representative, and as such also responsible for the Guest Observers (GO) Programme. M.N.G. does not relay proprietary information between the GO and Guaranteed Time Observation (GTO) Programmes, and does not decide on the definition and target selection of the GTO Programme. M.L. acknowledges support of the Swiss National Science Foundation under grant number PCEFP2_194576. M.F. and C.M.P. gratefully acknowledge the support of the Swedish National Space Agency (DNR 65/19, 174/18). D.G. gratefully acknowledges financial support from the CRT foundation under Grant No. 2018.2323 “Gaseous or rocky? Unveiling the nature of small worlds”. Y.A. acknowledges support from the Swiss National Science Foundation (SNSF) under grant 200020_192038. We acknowledge financial support from the Agencia Estatal de Investigación of the Ministerio de Ciencia e Innovación MCIN/AEI/10.13039/501100011033 and the ERDF “A way of making Europe” through projects PID2019-107061GB-C61, PID2019-107061GB-C66, PID2021-125627OB-C31, and PID2021-125627OB-C32, from the Centre of Excellence “Severo Ochoa” award to the Instituto de Astrofísica de Canarias (CEX2019-000920-S), from the Centre of Excellence “María de Maeztu” award to the Institut de Ciències de l’Espai (CEX2020-001058-M), and from the Generalitat de Catalunya/CERCA programme. We acknowledge financial support from the Agencia Estatal de Investigación of the Ministerio de Ciencia e Innovación MCIN/AEI/10.13039/501100011033 and the ERDF “A way of making Europe” through projects PID2019-107061GB-C61, PID2019-107061GB-C66, PID2021-125627OB-C31, and PID2021-125627OB-C32, from the Centre of Excellence “Severo Ochoa” award to the Instituto de Astrofísica de Canarias (CEX2019-000920-S), from the Centre of Excellence “María de Maeztu” award to the Institut de Ciències de l’Espai (CEX2020-001058-M), and from the Generalitat de Catalunya/CERCA programme. S.C.C.B. acknowledges support from FCT through FCT contracts nr. IF/01312/2014/CP1215/CT0004. C.B. acknowledges support from the Swiss Space Office through the ESA PRODEX program. A.C.C. acknowledges support from STFC consolidated grant numbers ST/R000824/1 and ST/V000861/1, and UKSA grant number ST/R003203/1. A.C.M.C. acknowledges support from the FCT, Portugal, through the CFisUC projects UIDB/04564/2020 and UIDP/04564/2020, with DOI identifiers 10.54499/UIDB/04564/2020 and 10.54499/UIDP/04564/2020, respectively. P.E.C. is funded by the Austrian Science Fund (FWF) Erwin Schrodinger Fellowship, program J4595-N. This project was supported by the CNES. The Belgian participation to CHEOPS has been supported by the Belgian Federal Science Policy Office (BELSPO) in the framework of the PRODEX Pro-

gram, and by the University of Liège through an ARC grant for Concerted Research Actions financed by the Wallonia-Brussels Federation. L.D. thanks the Belgian Federal Science Policy Office (BELSPO) for the provision of financial support in the framework of the PRODEX Programme of the European Space Agency (ESA) under contract number 4000142531. This work was supported by FCT – Fundação para a Ciência e a Tecnologia through national funds and by FEDER through COMPETE2020 through the research grants UIDB/04434/2020, UIDP/04434/2020, 2022.06962.PTDC. O.D.S.D. is supported in the form of work contract (DL 57/2016/CP1364/CT0004) funded by national funds through FCT. B.-O.D. acknowledges support from the Swiss State Secretariat for Education, Research and Innovation (SERI) under contract number MB22.00046. This project has received funding from the Swiss National Science Foundation for project 200021_200726. It has also been carried out within the framework of the National Centre of Competence in Research PlanetS supported by the Swiss National Science Foundation under grant 51NF40_205606. The authors acknowledge the financial support of the SNSF. M.G. is an F.R.S.-FNRS Senior Research Associate. Ch.H. acknowledges support from the European Union H2020-MSCA-ITN-2019 under Grant Agreement no. 860470 (CHAMELEON). S.H. gratefully acknowledges CNES funding through the grant 837319. J.K. gratefully acknowledges the support of the Swedish Research Council (VR: Etableringsbidrag 2017-04945). A.C., A.D., B.E., K.G., and J.K. acknowledge their role as ESA-appointed CHEOPS Science Team Members. K.W.F.L. was supported by Deutsche Forschungsgemeinschaft grants RA714/14-1 within the DFG Schwerpunkt SPP 1992, Exploring the Diversity of Extrasolar Planets. This work was granted access to the HPC resources of MesoPSL financed by the Region Ile de France and the project Equip@Meso (reference ANR-10-EQPX-29-01) of the programme Investissements d’Avenir supervised by the Agence Nationale pour la Recherche. P.M. acknowledges support from STFC research grant number ST/R000638/1. This work was also partially supported by a grant from the Simons Foundation (PI Queloz, grant number 327127). N.C.S. acknowledges funding by the European Union (ERC, FIERCE, 101052347). Views and opinions expressed are however those of the author(s) only and do not necessarily reflect those of the European Union or the European Research Council. Neither the European Union nor the granting authority can be held responsible for them. A.S. acknowledges support from the Swiss Space Office through the ESA PRODEX program. S.G.S. acknowledges support from FCT through FCT contract nr. CEECIND/00826/2018 and POPH/FSE (EC). The Portuguese team thanks the Portuguese Space Agency for the provision of financial support in the framework of the PRODEX Programme of the European Space Agency (ESA) under contract number 4000142255. Gy.M.S. acknowledges the support of the Hungarian National Research, Development and Innovation Office (NKFIH) grant K-125015, a PRODEX Experiment Agreement No. 4000137122, the Lendulet LP2018-7/2021 grant of the Hungarian Academy of Science and the support of the city of Szombathely. V.V.G. is an F.R.S.-FNRS Research Associate. J.V. acknowledges support from the Swiss National Science Foundation (SNSF) under grant PZ00P2_208945. N.A.W. acknowledges UKSA grant ST/R004838/1. T.W. acknowledges support from the UKSA and the University of Warwick.

References

- Akinsanmi, B., Santos, N. C., Faria, J. P., et al. 2020, *A&A*, **635**, L8
 Alam, M. K., Kirk, J., Dressing, C. D., et al. 2022, *ApJ*, **927**, L5
 Becker, J. C., Vanderburg, A., Rodriguez, J. E., et al. 2019, *AJ*, **157**, 19
 Belkovski, M., Becker, J., Howe, A., et al. 2022, *AJ*, **163**, 277
 Benz, W., Broeg, C., Fortier, A., et al. 2021, *Exp. Astron.*, **51**, 109
 Berard, D., Crossfield, I. J. M., Werner, M., et al. 2019, *AJ*, **157**, 185
 Borsato, L., Marzari, F., Nascimbeni, V., et al. 2014, *A&A*, **571**, A38
 Borsato, L., Malavolta, L., Piotto, G., et al. 2019, *MNRAS*, **484**, 3233
 Borsato, L., Piotto, G., Gandolfi, D., et al. 2021, *MNRAS*, **506**, 3810
 Bryant, E. M., Bayliss, D., Santerne, A., et al. 2021, *MNRAS*, **504**, L45
 Cosentino, R., Lovis, C., Pepe, F., et al. 2012, in *Ground-based and Airborne Instrumentation for Astronomy IV*, eds. I. S. McLean, S. K. Ramsay, & H. Takami, *SPIE Conf. Ser.*, **8446**, 84461V
 Edwards, B., Changeat, Q., Tsias, A., et al. 2023, *ApJS*, **269**, 31
 Garai, Z., Osborn, H. P., Gandolfi, D., et al. 2023, *A&A*, **674**, A44
 Grouffal, S., Santerne, A., Bourrier, V., et al. 2022, *A&A*, **668**, A172
 Harada, C. K., Dressing, C. D., Alam, M. K., et al. 2023, *AJ*, **166**, 208
 Holt, J. R. 1893, *A&A*, **12**, 646
 Hoyer, S., Guterman, P., Demangeon, O., et al. 2020, *A&A*, **635**, A24
 Kipping, D. M. 2010, *MNRAS*, **407**, 301
 Lund, M. N., Knudstrup, E., Silva Aguirre, V., et al. 2019, *AJ*, **158**, 248
 Maxted, P. F. L., Ehrenreich, D., Wilson, T. G., et al. 2022, *MNRAS*, **514**, 77
 Mayor, M., Pepe, F., Queloz, D., et al. 2003, *Messenger*, **114**, 20
 McLaughlin, D. B. 1924, *ApJ*, **60**, 22
 Osborn, H. P., Bonfanti, A., Gandolfi, D., et al. 2022, *A&A*, **664**, A156

- Osborn, H. P., Nowak, G., Hébrard, G., et al. 2023, *MNRAS*, **523**, 3069
- Psaridi, A., Osborn, H., Bouchy, F., et al. 2024, *A&A*, **685**, A5
- Rauer, H., Catala, C., Aerts, C., et al. 2014, *Exp. Astron.*, **38**, 249
- Rossiter, R. A. 1924, *ApJ*, **60**, 15
- Saillenfest, M., Sulis, S., Charpentier, P., & Santerne, A. 2023, *A&A*, **675**, A174
- Santerne, A., Malavolta, L., Kosiarek, M. R., et al. 2019, arXiv e-prints [arXiv:1911.07355]
- Tuson, A., Queloz, D., Osborn, H. P., et al. 2023, *MNRAS*, **523**, 3090
- Ulmer-Moll, S., Osborn, H. P., Tuson, A., et al. 2023, *A&A*, **674**, A43
- Vanderburg, A., Becker, J. C., Kristiansen, M. H., et al. 2016, *ApJ*, **827**, L10
- Winn, J. N. 2010, in *Exoplanets*, ed. S. Seager, 55
-
- ¹ Aix Marseille Univ, CNRS, CNES, LAM, 38 rue Frédéric Joliot-Curie, 13388 Marseille, France
e-mail: sophia.sulis@lam.fr
- ² INAF, Osservatorio Astronomico di Padova, Vicolo dell'Osservatorio 5, 35122 Padova, Italy
- ³ Université Aix Marseille, CNRS, CNES, LAM, Marseille, France
- ⁴ Center for Space and Habitability, University of Bern, Gesellschaftsstrasse 6, 3012 Bern, Switzerland
- ⁵ Department of Physics and Kavli Institute for Astrophysics and Space Research, Massachusetts Institute of Technology, Cambridge, MA 02139, USA
- ⁶ Department of Astronomy, Stockholm University, AlbaNova University Center, 10691 Stockholm, Sweden
- ⁷ European Space Agency (ESA), European Space Research and Technology Centre (ESTEC), Keplerlaan 1, 2201 AZ Noordwijk, The Netherlands
- ⁸ Observatoire astronomique de l'Université de Genève, Chemin Pegasi 51, 1290 Versoix, Switzerland
- ⁹ Leiden Observatory, University of Leiden, PO Box 9513, 2300 RA Leiden, The Netherlands
- ¹⁰ Department of Space, Earth and Environment, Chalmers University of Technology, Onsala Space Observatory, 439 92 Onsala, Sweden
- ¹¹ Dipartimento di Fisica, Università degli Studi di Torino, Via Pietro Giuria 1, 10125 Torino, Italy
- ¹² Weltraumforschung und Planetologie, Physikalisches Institut, University of Bern, Gesellschaftsstrasse 6, 3012 Bern, Switzerland
- ¹³ Instituto de Astrofísica de Canarias, Vía Láctea s/n, 38200 La Laguna, Tenerife, Spain
- ¹⁴ Departamento de Astrofísica, Universidad de La Laguna, Astrofísico Francisco Sanchez s/n, 38206 La Laguna, Tenerife, Spain
- ¹⁵ Admatis, 5. Kandó Kálmán Street, 3534 Miskolc, Hungary
- ¹⁶ Depto. de Astrofísica, Centro de Astrobiología (CSIC-INTA), ESAC campus, 28692 Villanueva de la Cañada (Madrid), Spain
- ¹⁷ Instituto de Astrofísica e Ciências do Espaço, Universidade do Porto, CAUP, Rua das Estrelas, 4150-762 Porto, Portugal
- ¹⁸ Departamento de Física e Astronomia, Faculdade de Ciências, Universidade do Porto, Rua do Campo Alegre, 4169-007 Porto, Portugal
- ¹⁹ Space Research Institute, Austrian Academy of Sciences, Schmiedlstrasse 6, 8042 Graz, Austria
- ²⁰ INAF – Osservatorio Astronomico di Padova, Padova, Italy
- ²¹ Centre for Exoplanet Science, SUPA School of Physics and Astronomy, University of St Andrews, North Haugh, St Andrews KY16 9SS, UK
- ²² CFisUC, Department of Physics, University of Coimbra, 3004-516 Coimbra, Portugal
- ²³ Institute of Planetary Research, German Aerospace Center (DLR), Rutherfordstrasse 2, 12489 Berlin, Germany
- ²⁴ INAF, Osservatorio Astrofisico di Torino, Via Osservatorio, 20, 10025 Pino Torinese To, Italy
- ²⁵ Centre for Mathematical Sciences, Lund University, Box 118, 221 00 Lund, Sweden
- ²⁶ Astrobiology Research Unit, Université de Liège, Allée du 6 Août 19C, 4000 Liège, Belgium
- ²⁷ Space sciences, Technologies and Astrophysics Research (STAR) Institute, Université de Liège, Allée du 6 Août 19C, 4000 Liège, Belgium
- ²⁸ Institute of Astronomy, KU Leuven, Celestijnenlaan 200D, 3001 Leuven, Belgium
- ²⁹ ELTE Gothard Astrophysical Observatory, Szent Imre herceg u. 112, 9700 Szombathely, Hungary
- ³⁰ SRON Netherlands Institute for Space Research, Niels Bohrweg 4, 2333 CA Leiden, The Netherlands
- ³¹ Centre Vie dans l'Univers, Faculté des sciences, Université de Genève, Quai Ernest-Ansermet 30, 1211 Genève 4, Switzerland
- ³² National and Kapodistrian University of Athens, Department of Physics, University Campus, Zografos, 157 84 Athens, Greece
- ³³ Department of Astrophysics, University of Vienna, Türkenschanzstrasse 17, 1180 Vienna, Austria
- ³⁴ Institute for Theoretical Physics and Computational Physics, Graz University of Technology, Petersgasse 16, 8010 Graz, Austria
- ³⁵ Konkoly Observatory, Research Centre for Astronomy and Earth Sciences, Konkoly Thege Miklós út 15-17, 1121 Budapest, Hungary
- ³⁶ ELTE Eötvös Loránd University, Institute of Physics, Pázmány Péter sétány 1/A, 1117 Budapest, Hungary
- ³⁷ Lund Observatory, Division of Astrophysics, Department of Physics, Lund University, Box 118, 22100 Lund, Sweden
- ³⁸ IMCCE, UMR8028 CNRS, Observatoire de Paris, PSL Univ., Sorbonne Univ., 77 av. Denfert-Rochereau, 75014 Paris, France
- ³⁹ Institut d'astrophysique de Paris, UMR7095 CNRS, Université Pierre & Marie Curie, 98bis Blvd. Arago, 75014 Paris, France
- ⁴⁰ Astrophysics Group, Lennard Jones Building, Keele University, Staffordshire ST5 5BG, UK
- ⁴¹ INAF, Osservatorio Astrofisico di Catania, Via S. Sofia 78, 95123 Catania, Italy
- ⁴² Institute of Optical Sensor Systems, German Aerospace Center (DLR), Rutherfordstrasse 2, 12489 Berlin, Germany
- ⁴³ Physikalisches Institut, University of Bern, Sidlerstrasse 5, 3012 Bern, Switzerland
- ⁴⁴ Dipartimento di Fisica e Astronomia "Galileo Galilei", Università degli Studi di Padova, Vicolo dell'Osservatorio 3, 35122 Padova, Italy
- ⁴⁵ Department of Physics, University of Warwick, Gibbet Hill Road, Coventry CV4 7AL, UK
- ⁴⁶ ETH Zurich, Department of Physics, Wolfgang-Pauli-Strasse 2, 8093 Zurich, Switzerland
- ⁴⁷ Cavendish Laboratory, JJ Thomson Avenue, Cambridge CB3 0HE, UK
- ⁴⁸ Institut fuer Geologische Wissenschaften, Freie Universitaet Berlin, Maltheserstrasse 74-100, 12249 Berlin, Germany
- ⁴⁹ Institut de Ciències de l'Espai (ICE, CSIC), Campus UAB, Can Magrans s/n, 08193 Bellaterra, Spain
- ⁵⁰ Institut d'Estudis Espacials de Catalunya (IEEC), Gran Capità 2-4, 08034 Barcelona, Spain
- ⁵¹ ELTE Eötvös Loránd University, Gothard Astrophysical Observatory, Szent Imre h. u. 112, 9700 Szombathely, Hungary
- ⁵² HUN-REN-ELTE Exoplanet Research Group, Szent Imre h. u. 112, Szombathely 9700, Hungary
- ⁵³ Institute of Astronomy, University of Cambridge, Madingley Road, Cambridge CB3 0HA, UK